Sterile neutrinos: Direct mixing effects versus induced mass matrix of active neutrinos

Alexei Yu. Smirnov[1,2,*] and Renata Zukanovich Funchal[1,3,†]

[1]*ICTP, Strada Costiera 11, 34014 Trieste, Italy*
[2]*Institute for Nuclear Research, Russian Academy of Sciences, Moscow, Russia*
[3]*Instituto de Física, Universidade de São Paulo, C. P. 66.318, 05315-970 São Paulo, Brazil*
(Received 7 April 2006; published 5 July 2006)

Mixing of active neutrinos with sterile ones generate "induced" contributions to the mass matrix of active neutrinos $\sim m_S \sin^2\theta_{aS}$, where m_S is the Majorana mass of the sterile neutrino and θ_{aS} is the active-sterile mixing angle. We study possible effects of the induced matrix which can modify substantially the implications of neutrino oscillation results. We have identified the regions of m_S and $\sin^2\theta_{aS}$ where the induced matrix (i) provides the dominant structures, (ii) gives the subdominant effects, and (iii) where its effects can be neglected. The induced matrix can be responsible for peculiar properties of the lepton mixing and neutrino mass spectrum, in particular, it can generate the tribimaximal mixing. We update and discuss bounds on the induced masses from laboratory measurements, astrophysics, and cosmology. We find that substantial impact of the induced matrix is possible if $m_S \sim (0.1$–$0.3)$ eV and $\sin^2\theta_{aS} \sim 10^{-3}$–$10^{-2}$ or $m_S \geq 300$ MeV and $\sin^2\theta_{aS} \leq 10^{-9}$. The bounds can be relaxed in cosmological scenarios with low reheating temperature, if sterile neutrinos decay sufficiently fast, or their masses change with time.

I. INTRODUCTION

There are two salient properties of neutrinos related to neutrality which distinguish them from other known fermions:
  (i) the possibility to have a Majorana mass term;
  (ii) mix with new fermions which are singlets of the standard model (SM) symmetry group.
So it would seem natural to explain unusual properties of neutrinos, such as smallness of masses and large mixing, using these two features. In fact, the seesaw mechanism [1] employs both.

It may happen however that the seesaw mechanism is not enough to explain the pattern of the lepton mixing, especially if quark-lepton symmetry or unification are imposed. In this connection, we will concentrate on the second feature—the possibility of neutrinos to mix with singlets of the standard model, i.e., sterile neutrinos. In general, sterile neutrinos may originate from some other sectors of the theory, e.g. related to supersymmetry breaking or extra dimensions, and not coincide with the right-handed components of neutrino fields.

In all, there are two types of effects of the mixing:
  (i) Direct effects—when new states can be produced in various processes and participate in neutrino oscillations, etc.;
  (ii) Indirect effects—via the modification of the mass matrix of light active neutrinos.
The role and relevance of these effects is determined by masses and mixings of sterile neutrinos. In some ranges of

parameters the cosmological and astrophysical consequences of mixing are more important and the influence on the mass matrix is negligible. In other regions vice versa: direct mixing effects are negligible—mixing becomes "invisible" but the modification of the mass matrix is substantial.

Being light, sterile neutrinos can immediately take part in the phenomenology of neutrino oscillations changing the interpretation of experimental results [2–4]. Being heavy and weakly mixed, they do not show up in oscillations and other processes, however their invisible mixing can strongly modify the mass matrix of active neutrinos and therefore change implications of neutrino results for theory. In particular, in this way, the presence of sterile neutrinos can induce the large or maximal mixing of the active neutrino components [5,6], or, for instance, produce deviation of the 1–2 mixing from maximal [7].

In a range of masses $m_S < Q$, where Q is the energy release in processes, sterile neutrinos do not decouple since they still can be produced. They can decouple here in the sense that their direct dynamical effects are negligible due to the smallness of mixing. For bigger masses, $m_S > Q$, sterile neutrinos decouple, as it happens in the standard seesaw mechanism. This decoupling generates an additional contribution to the mass matrix of active neutrinos and gives negligible deviation from universality.

From the observational point of view until now there is no clear evidence of existence of sterile neutrinos, though some hints exist. Those include, the liquid scintillator neutrino detector (LSND) result [8] and its interpretation in terms of oscillations in the $(3 + 1)$ or $(3 + 2)$ neutrino mixing schemes; large scale structure formation in the Universe with the warm dark matter composed of the

_____

*Electronic address: smirnov@ictp.it
†Electronic address: zukanov@if.usp.br

keV sterile neutrinos [9,10]; high observed velocities of pulsars and their explanation as an asymmetric emission of the keV sterile neutrinos [11]; the early reionization of the Universe due to the radiative S-decay [12].

In this paper we study in detail the possible effects of sterile-active mixing on the mass matrix of active neutrinos. We obtain bounds on these induced masses from the direct mixing effects. We find the impact of the induced matrix may be considerable if $m_S \sim (0.1\text{--}0.3)$ eV and $\sin^2\theta_{aS} \sim 10^{-3}\text{--}10^{-2}$ or $m_S \gtrsim 300$ MeV and $\sin^2\theta_{aS} \lesssim 10^{-9}$.

The paper is organized as follows. In Sec. II, we determine the mass matrix induced by the mixing of active neutrinos with a sterile one. We study the properties of the induced mass matrix and the possibility to explain certain features of the neutrino mass spectrum and mixing pattern using this matrix. We find values of mixing (as a function of the mass of the sterile component) for which the effect of the sterile neutrino (i) explains the dominant structures of the mass matrix; (ii) produces the subdominant structures of the mass matrix; (iii) can be neglected, being of the order or below the 1σ uncertainties of the present measurements. In Sec. III, we consider various bounds on masses and mixing of the sterile neutrino and consequently, on the induced matrix, in particular, those from astrophysics and cosmology. We then, in Sec. IV, confront these bounds with regions found in Sec. II and discuss how they can be improved in the future. We also comment on new physics scenarios which allow to evade the bounds. Our conclusions are given in Sec. V.

II. ACTIVE-STERILE MIXING AND INDUCED MASS MATRIX

A. Induced mass matrix

Let us consider three active Majorana neutrinos $\nu_a = (\nu_e, \nu_\mu, \nu_\tau)^T$ with mass matrix

$$\mathbf{m_a} = \begin{pmatrix} m_{ee} & m_{e\mu} & m_{e\tau} \\ m_{\mu e} & m_{\mu\mu} & m_{\mu\tau} \\ m_{\tau e} & m_{\tau\mu} & m_{\tau\tau} \end{pmatrix} \quad (1)$$

generated, e.g., by the seesaw mechanism [1]. We consider $m_a \lesssim 1$ eV—below the present upper bound to avoid strong cancellations of different contributions.

We assume that (i) the active neutrinos mix with a single (for simplicity) sterile neutrino S, via the masses

$$m_{aS}^T \equiv (m_{eS}, m_{\mu S}, m_{\tau S}); \quad (2)$$

(ii) S has a Majorana mass m_S, which is much larger than the mixing masses and m_a:

$$m_S \gg m_{aS}, m_a. \quad (3)$$

So, in the basis (ν_a, S), the complete mass matrix has the form

$$\begin{pmatrix} \mathbf{m_a} & m_{aS} \\ m_{aS}^T & m_S \end{pmatrix}. \quad (4)$$

Properties of S: masses, mixing, possible new symmetries, etc., are determined by some new physics which, in general, differs from physics responsible for the generation of $\mathbf{m_a}$.

Under condition (3) the block diagonalization gives for the light neutrinos the mass matrix

$$\mathbf{m}_\nu \approx \mathbf{m_a} + \mathbf{m_I}, \quad (5)$$

where

$$\mathbf{m_I} \equiv -\frac{1}{m_S}(m_{aS}) \times (m_{aS})^T, \quad (6)$$

is the *induced contribution* to the neutrino mass matrix due to active-sterile mixing, or shortly, *induced mass matrix*. For the individual matrix element we have

$$(m_\nu)_{ij} = (m_a)_{ij} - \frac{m_{iS}m_{jS}}{m_S}. \quad (7)$$

Let us introduce the active-sterile mixing angles

$$\sin\theta_{jS} \approx \frac{m_{jS}}{m_S}. \quad (8)$$

Then the induced masses can be written as

$$(m_I)_{ij} = -\sin\theta_{iS}\sin\theta_{jS}m_S. \quad (9)$$

It is this combination of parameters which determines physical effects. For the flavor blind mixing we would have simply the product $\sin^2\theta_S m_S$.

In the case of a single sterile neutrino the induced contribution is the singular (rank-1) matrix. This feature substantially restricts possible effects of the induced matrix. In the case of two (several) sterile neutrinos, two (several) independent singular contributions to the induced matrix appear:

$$\mathbf{m_I} = -\sum_i \frac{1}{m_S^{(i)}}(m_{aS}^{(i)}) \times (m_{aS}^{(i)})^T. \quad (10)$$

That opens new possibilities in the description of neutrino mass matrices. Apparently, with three neutrinos any structure of the matrix can be reproduced.

B. Neutrino mass matrix in flavor basis

To evaluate the impact of the active-sterile mixing, we reconstruct the neutrino mass matrix from the data in the flavor basis in the context of three active neutrinos. The values of matrix elements in terms of the oscillation parameters are given by

$$m_{\alpha\beta} = m_1 e^{-i2\lambda_1} U_{\alpha 1}^* U_{\beta 1}^* + m_2 U_{\alpha 2}^* U_{\beta 2}^* + m_3 e^{-i2\lambda_3} U_{\alpha 3}^* U_{\beta 3}^* \quad (11)$$

with $\alpha, \beta = e, \mu, \tau$, and $U_{\alpha i}$ being the elements of the

Pontecorvo-Maki-Nakagawa-Sakata (PMNS) matrix. The matrix elements $U_{\alpha i}$ are functions of the three mixing angles θ_{12}, θ_{13}, θ_{23} and the complex phase δ given by the standard parametrization of the mixing matrix.

We use the best fit values and 1σ intervals of the oscillation parameters from Ref. [13]:

$$|\Delta m^2_{32}| = 2.4(1.00^{+0.11}_{-0.13}) \times 10^{-3} \text{ eV}^2, \qquad (12)$$

$$\Delta m^2_{21} = 7.92(1.00 \pm 0.045) \times 10^{-5} \text{ eV}^2, \qquad (13)$$

$$\sin^2\theta_{23} = 0.44(1.00^{+0.21}_{-0.11}), \qquad (14)$$

$$\sin^2\theta_{12} = 0.314(1.00^{+0.09}_{-0.075}), \qquad (15)$$

and for $\sin^2\theta_{13}$ we take

$$\sin^2\theta_{13} = 0.9(1.0^{+3.1}_{-0.9}) \times 10^{-2} \qquad (16)$$

with the nonzero best fit value.

The reconstructed matrices for the normal, inverted mass hierarchy and the degenerate mass spectrum are given in Table I, where we show the absolute values of the matrix elements. For each case we present (i) the matrix for the best fit values of the parameters, (ii) the intervals which correspond to the 1σ experimental uncertainties for zero CP phases and the intervals when also the CP-violating phases vary in the whole possible range: $\lambda_i = 0 - \pi$, $\delta = 0 - \pi/2$.

The following comments are in order.

(1) In the case of normal mass hierarchy we take $m_1 = 0$, so that $m_2 = \sqrt{\Delta m^2_{21}}$ and $m_3 = \sqrt{\Delta m^2_{31}}$. Notice that the 1-3 element of the matrix is much smaller than the 1-2 element and elements of the dominant block are different. This is the consequence of nonzero (though statistically insignificant) 1-3 mixing and shift of the 2-3 mixing from the maximal one. The 1σ experimental uncertainties lead to $\delta m_{ee} \sim 2.5$ meV, $\delta m_{e\mu} \sim \delta m_{e\tau} \sim \delta m_{\mu\tau} \sim 5$ meV, $\delta m_{\mu\mu} \sim \delta m_{\tau\tau} \sim 10$ meV. The effect of CP

phases is subleading. Variations of phases λ_3, δ result in similar size of the intervals and both effects double the indicated uncertainties.

Notice that there are strong correlations between elements, so that their values cannot be taken from the indicated intervals independently.

(2) For the inverted hierarchy we take $m_3 = 0$, $m_1 \approx m_2 \approx \sqrt{|\Delta m^2_{31}|}$. We choose $\lambda_1 = \delta = 0$ (λ_3 is irrelevant) for the best fit data analysis. The 1σ experimental uncertainties lead to $\delta m \sim (8-10)$ meV for all matrix elements but $\delta m_{\mu\tau} \sim 4$ meV. The effect of phase variations is much stronger. Now the phases affect the dominant block and therefore $\delta m \sim m$.

(3) Degenerate spectrum. For illustration we take $m_1 \approx m_2 \approx m_3 = m_0 = 0.2$ eV. The experimental errors produce very small effect: $\delta m \sim 1$ meV. In contrast, effects of phase variations are very strong, $\delta m \sim m_0$. Here also variations (values) of different elements are strongly correlated.

C. Induced matrix and the dominant structures

The mass and mixing patterns in quark and lepton sectors are strongly different. The difference can (at least partially) originate from the active-sterile mixing which is absent in the quark sector. The shortcoming of this proposal is the coincidence problem: two different contributions to the mass matrix, active $\mathbf{m_a}$ and induced $\mathbf{m_I}$, are of the same order or within $1-2$ orders of magnitude in spite of the fact that they have different, and at the first sight, unrelated origins. The only argument in favor is that this will be not the only case—we meet the coincidence problem in other areas too. Another possibility is that $\mathbf{m_I} \gg \mathbf{m_a}$.

Let us consider first the case of one sterile neutrino. Because of the singular (rank 1) character of the induced matrix it cannot reproduce the dominant structures of the neutrino mass matrix in the case of the degenerate mass spectrum and inverted mass hierarchy. In the former case

TABLE I. The reconstructed matrices for the normal and inverted mass hierarchies as well as the degenerate mass spectrum for $m_0 = 0.2$ eV. The moduli of elements are given in units of 1 meV. For each case we present: the matrix for the best fit values of the mixing parameters, the intervals of the matrix elements obtained varying the experimental values within 1σ for $\delta = \lambda_3 = 0$, and also for free CP-violating phases.

Case	Best Fit $\delta = \lambda_3 = 0$			Experimentally allowed at 1σ $\delta = \lambda_3 = 0$			Free CP phases		
Normal	3.2	6.0	0.6	2.5–5.0	2.7–9.8	0.–5.1	0.3–5.0	0.–10.8	0.–11.1
		24.8	21.4		19.9–30.3	18.1–22.9		12.7–30.9	18.5–29.4
			30.7			24.5–34.0			16.7–34.5
Inverted	48.0	2.8	3.7	43.2–51.0	0.–8.6	0.–9.2	11.4–51.0	0.–39.0	0.–36.7
		27.4	24.0		21.3–31.9	21.3–25.6		0.–32.1	4.6–26.7
			21.7			17.8–28.2			0.–28.2
Degenerate	200.0	0.5	0.4	200.1–200.3	0.06–1.0	0.–1.0	60.0–200.3	0.–176.6	0.–170.3
		202.7	2.9		202.1–203.6	2.4–3.3		0.02–203.6	0.5–200.3
			203.5			202.5–204.1			0.02–204.1

det$\mathbf{m} \approx m_0^3$, where m_0 is the scale of neutrino mass. In the latter—there are two dominant eigenvalues and the determinant of the 1-2 submatrix is nonzero.

Essentially this means that the matrix induced by one sterile neutrino can be the origin of the dominant block *only* in the case of normal mass hierarchy. This can explain the large (maximal) 2-3 mixing. Suppose

$$m_{\mu S} = m_{\tau S} = m_0, \qquad m_{eS} \ll m_0, \qquad (17)$$

then

$$\mathbf{m_I} \approx \frac{m_0^2}{m_S} \begin{pmatrix} 0 & 0 & 0 \\ 0 & 1 & 1 \\ 0 & 1 & 1 \end{pmatrix}. \qquad (18)$$

From (18) we obtain $2m_0^2/m_S = \sqrt{\Delta m_{\text{atm}}^2}$ or

$$m_S \sin^2\theta_S = 0.5\sqrt{\Delta m_{\text{atm}}^2} \approx 25 \text{ meV}. \qquad (19)$$

Parameters of the 1-2 block (mixing and mass) should be given by the original active mass matrix. For the best fit values of the oscillation parameters (here we take $\sin^2\theta_{13} = 0$) and the induced matrix (18) the active neutrino mass matrix should be of the form

$$\mathbf{m_a} = U_{23}^m U_{12}^{\text{sol}} \mathbf{m_2} U_{12}^{\text{sol}T} U_{23}^{mT} = m_2 \begin{pmatrix} s^2 & \frac{sc}{\sqrt{2}} & -\frac{sc}{\sqrt{2}} \\ \cdots & \frac{c^2}{2} & -\frac{c^2}{2} \\ \cdots & \cdots & \frac{c^2}{2} \end{pmatrix}, \qquad (20)$$

where $\mathbf{m_2} = \text{diag}(0, m_2, 0)$, $s \equiv \sin\theta_{12}$, $c \equiv \cos\theta_{12}$, U_{12}^{sol} is the 1-2 rotation matrix on the solar mixing angle, U_{23}^m is the matrix of maximal 2-3 mixing. We assumed that $m_1 \approx 0$. Notice that all elements of this matrix are nearly equal being in the range 0.31–0.35.

A nonzero m_1 would be the equivalent of adding to (20) the matrix $m_1\mathbf{I}$ proportional to the unit matrix and substituting $m_2 \to (m_2 - m_1)$, if there is no CP-violating phases. That does not change our conclusion provided that $m_1 \ll m_2$.

The induced matrix can be chosen in such a way that the active one has hierarchical structure with small mixings similar to the charged fermion mass matrices. (Partly this case has been studied in [6]). Consider nonuniversal active-sterile coupling of the type

$$m_{\alpha S} = \sqrt{(m_3 - m_1)m_S}(\alpha, a, b), \qquad \alpha \ll a \sim b. \quad (21)$$

Then the required mass matrix of active neutrinos can be written as

$$\mathbf{m_a} = m_1\mathbf{I} + (m_3 - m_1)$$
$$\times \begin{pmatrix} \epsilon s^2 - \alpha^2 & \epsilon\frac{sc}{\sqrt{2}} - \alpha a & -\epsilon\frac{sc}{\sqrt{2}} - \alpha b \\ \cdots & 1 - a^2 + \epsilon\frac{c^2}{2} & 1 - ab - \epsilon\frac{c^2}{2} \\ \cdots & \cdots & 1 - b^2 + \epsilon\frac{c^2}{2} \end{pmatrix}, \qquad (22)$$

where $\epsilon \equiv m_2/(m_3 - m_1)$. For $a = 0.95$ and $b = 1.50$ we obtain hierarchical 2-3 block with $(m_a)_{22}:(m_a)_{23}:(m_a)_{33} \approx 0.1:0.4:1.2$. Other elements are of the order $0.02-0.04$ if $\alpha \sim 0.01$. Certain hierarchy among those elements can be obtained for nonzero 1-3 mixing and some deviation of the 2-3 mixing from the maximal. The overall spread of the values of elements by 2 orders of magnitude can be easily obtained.

Another scenario (essentially considered in [6]) is that $b \gg a$, so that the induced matrix corrects the 33 element only. Taking, e.g., $m_{33} = \sin^2\theta_{\tau S}m_S \sim 300$ meV and the final matrix $\mathbf{m}_\nu$ as in the Table I, we obtain that the original active mass matrix should be like that for normal hierarchy (Table I) but with $m_{33} \sim 300$ meV, that is, strongly hierarchical.

D. Induced matrix and mass hierarchy

An interesting possibility is that the induced matrix can switch the mass hierarchy from normal to inverted and vice versa. Indeed,

$$\mathbf{m}_\nu^{\text{inv}} \sim \sqrt{2}\mathbf{m}_\nu^{\text{norm}} - \sqrt{\frac{|\Delta m_{32}^2|}{2}}\mathbf{D}, \qquad (23)$$

where the induced term $\mathbf{D}$ is close to the "democratic" matrix with all elements being nearly 1.

E. Induced matrix and tribimaximal mixing

The mass matrix which generates the tribimaximal mixing in the normal mass hierarchy case can be presented as

$$\mathbf{m} = \frac{\sqrt{|\Delta m_{32}^2|}}{2} \begin{pmatrix} 0 & 0 & 0 \\ 0 & 1 & -1 \\ 0 & -1 & 1 \end{pmatrix} + \frac{\sqrt{\Delta m_{21}^2}}{3} \begin{pmatrix} 1 & 1 & 1 \\ 1 & 1 & 1 \\ 1 & 1 & 1 \end{pmatrix}. \qquad (24)$$

It is the sum of two singular matrices. The subdominant (second) matrix can be induced by universal mixing with the sterile component

$$m_{\alpha S} = m_0(1, 1, 1). \qquad (25)$$

Then according to (24)

$$m_S \sin^2\theta_S = \frac{\sqrt{\Delta m_{21}^2}}{3} \approx 3 \text{ meV}. \qquad (26)$$

In fact, both matrices in (24) can be induced by the active-sterile mixing, if the second sterile neutrino is introduced with mixing elements

$$m'_{\alpha S} = m_0(0, 1, -1). \tag{27}$$

In this case the original active neutrino masses should be very small, e.g., of the order of the Planck mass suppressed scale: $\sim v^2_{\mathrm{EW}}/M_{\mathrm{Pl}}$.

F. Induced matrix and QLC

If not accidental, the quark-lepton complementarity (QLC) relation [14] can imply that (i) there is some structure in the lepton sector which generates the bimaximal mixing $U_{\mathrm{bm}} \equiv U^m_{23} U^m_{12}$; and (ii) there is the quark-lepton symmetry which "propagates" the Cabibbo-Kobayashi-Maskawa (CKM)-type rotations to the lepton sector.

Let us consider a possibility that the induced matrix is responsible for the bimaximal mixing:

$$\mathbf{m_I} = \mathbf{m_{bm}} = U_{\mathrm{bm}}\mathbf{m^{diag}}U^T_{\mathrm{bm}}, \tag{28}$$

whereas the charged lepton mass matrix produces the CKM-type rotation. The original active neutrino matrix should then give a very small contribution.

Clearly this scenario cannot be realized with only one sterile neutrino: Taking $\mathbf{m^{diag}} = \mathbf{diag}(0, 0, m_3)$ we find that $\mathbf{m_I} = U^m_{23}\mathbf{m_3}U^{mT}_{23}$ with a single maximal mixing. With two sterile neutrinos the matrix $\mathbf{m_{bm}}$ which generates the bimaximal mixing can be reproduced precisely. As an example one can take $m_{\alpha S} = m_0(a, b, -b)$ and $m'_{\alpha S} = m_0(0, x, y)$, where $x = \sqrt{d + 0.5a^2 - b^2}$, $y = (d - 0.5a^2 + b^2)/x$, and a, b, d are free parameters.

G. Small and negligible induced contribution

The induced matrix becomes irrelevant if

$$\frac{m_{iS}m_{jS}}{m_S} \ll (m_a)_{ij}. \tag{29}$$

Let us find conditions under which the effects of the sterile neutrino are below the present 1σ spread of the matrix elements. Uncertainties depend on the type of mass spectra and are different for different elements.

For the normal mass hierarchy the effects are below 1σ if

$$\sin^2\theta_{eS}m_S < 2 \text{ meV}, \qquad \sin^2\theta_{\mu S}m_S, \\ \sin^2\theta_{\tau S}m_S < 5 \text{ meV}. \tag{30}$$

For μ and τ we have taken the uncertainty of $m_{\mu\tau}$ which is the smallest one.

For the inverted hierarchy the induced contributions are below 1σ uncertainties if

$$\sin^2\theta_{eS}m_S < 8 \text{ meV}, \qquad \sin^2\theta_{\mu S}m_S < 4 \text{ meV}. \tag{31}$$

Larger effects of sterile neutrinos, $\sin^2\theta_S m_S < 20$ meV, can be mimicked by the phase variations.

In the case of degenerate spectrum 1σ experimental uncertainties restrict

$$\sin^2\theta_{eS}m_S < 1 \text{ meV}. \tag{32}$$

The phase change produces the same effect as sterile neutrinos with $\sin^2\theta_{\alpha S}m_S \sim 200$ meV.

Sterile neutrinos can be responsible for fine structures of the mass matrix. The smallest (observable) structure is related to the solar mass split. In the case of inverted hierarchy this would correspond to the contribution $\sin^2\theta_{eS}m_S \sim 1.5$ meV, and for the degenerate mass spectrum we obtain the smallest quantity: $\sin^2\theta_{eS}m_S \sim 0.4$ meV.

So, we can identify three benchmarks:

(1) For sterile neutrinos with mixings and masses smaller than

$$\sin^2\theta_{\alpha S}m_S = 1 \text{ meV} \tag{33}$$

the effects are below the present 1σ experimental uncertainties for the hierarchical spectra. Still these neutrinos can influence the subleading structures in the case of the degenerate spectrum.

(2) Sterile neutrinos with

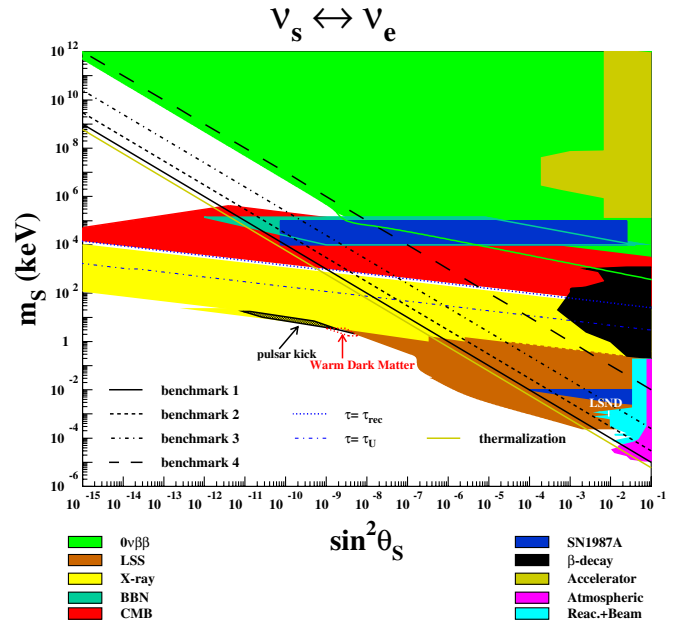$$\sin^2\theta_{\alpha S}m_S = 3 \text{ meV} \tag{34}$$

FIG. 1 (color online). The benchmark lines Eqs. (33), (35), and (55) versus the current astrophysical, cosmological and laboratory bounds on $\nu_S - \nu_e$ mixing as described in the text. The colored regions are excluded in each case. The thermalization line and the two decay lines $\tau_S = \tau_{\mathrm{rec}}$ and $\tau_S = \tau_U$ are also shown. We show also the allowed regions for the warm dark matter and the LSND $(3 + 1)$ as well as the region that could explain pulsar velocities.
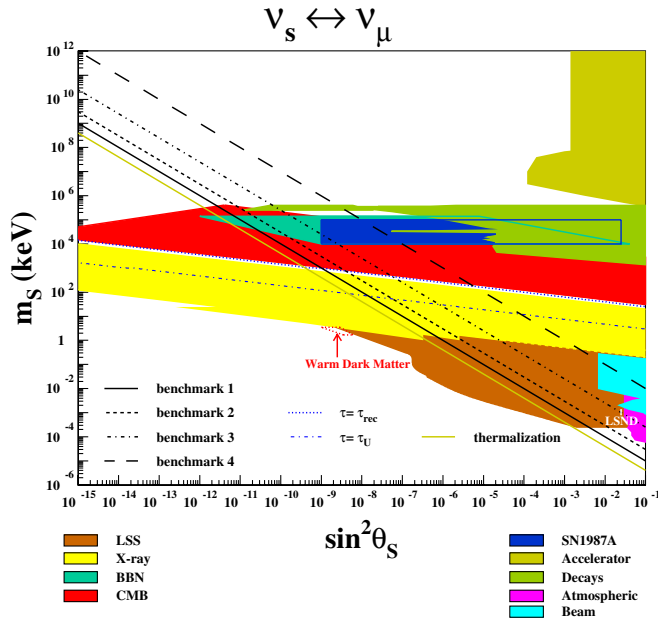
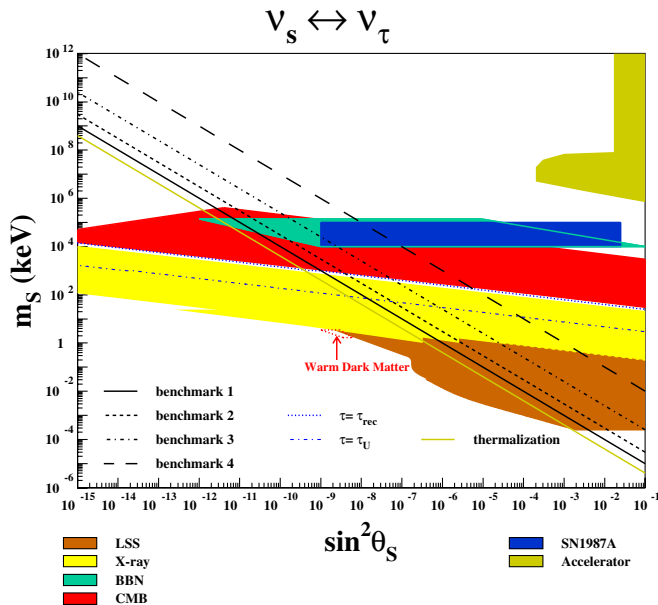FIG. 2 (color online). Same as Fig. 1 but for $\nu_S - \nu_\mu$ mixing.

can generate the subleading structures in the case of normal mass hierarchy.

(3) Sterile neutrinos with

$$\sin^2\theta_{\alpha S} m_S = (20\text{--}30) \text{ meV} \quad (35)$$

can generate dominant structures in the case of normal and inverted hierarchies. For larger masses and mixings they can lead to dominant structures of the degenerate spectrum.

In Figs. 1–3 we show the lines of constant induced mass $\sin^2\theta_{\alpha S} m_S = \text{const.}$, in the plane $\sin^2\theta_{\alpha S}$ and m_S which correspond to the values in (33)–(35).

FIG. 3 (color online). Same as Fig. 1 but for $\nu_S - \nu_\tau$ mixing.

III. BOUNDS ON THE ACTIVE-STERILE MIXING

In this section we describe the direct mixing effects of S and bounds on its masses and mixings.

A. Production, thermalization, decay

The most stringent bounds follow from astrophysics and cosmology. Sterile neutrinos can be produced in the early Universe nonthermally through their mixing with active neutrinos, affecting primordial nucleosynthesis, cosmic microwave background radiation, as well as the growth of cosmological structures.

We assume that no primordial density of sterile neutrinos existed, and all sterile neutrinos were produced in the early Universe due to mixing with active neutrinos and oscillations [9,10].

The "thermalization" lines and the "decay" lines in the m_S-$\sin^2\theta_S$ plane (Figs. 1–3) allow to understand various bounds.

(1) The thermalization lines give the lower bounds of the m_S-$\sin^2\theta_S$ region where the sterile neutrinos are thermalized before the primordial nucleosynthesis. According to Refs. [15,16] the lines are slightly different for mixing with electron and nonelectron neutrinos:

$$m_S \sin^2\theta_S = 0.6 \text{ meV} \quad \text{for } \nu_e, \quad (36)$$

$$m_S \sin^2\theta_S = 0.4 \text{ meV} \quad \text{for } \nu_\mu, \nu_\tau. \quad (37)$$

Notice that the thermalization lines have the same functional dependence as the isolines of induced mass. Furthermore, the lines are below the benchmarks obtained in (33)–(35). That is, sterile neutrinos with parameters which give significant induced contribution were thermalized in the early Universe.

(2) We confront the lifetime of neutrinos with the time of recombination, $\tau_{\text{rec}} \approx 10^{12}$ s, and the age of the Universe, $\tau_U = 4 \times 10^{17}$ s. The decay rate of S strongly depends on m_S. For small m_S the main channel is $S \rightarrow 3\nu$ and then the following channels open: $S \rightarrow \nu + l + \bar{l}$, $S \rightarrow \nu + q + \bar{q}$, etc. The decay rate can be written as

$$\frac{1}{\tau_S} \approx \kappa(m_S)\Gamma_\mu \left(\frac{m_S}{m_\mu}\right)^5 \sin^2\theta_S, \quad (38)$$

where m_μ and Γ_μ are the muon mass and decay rate, correspondingly, and $\kappa(m_S)$ is the number of decay channels for a given value of m_S. So, for the nonrelativistic sterile neutrinos, the lines of constant decay rate are given by

$$\kappa(m_S) m_S^5 \sin^2\theta_S = \text{const.} \quad (39)$$

In Figs. 1–3 we show two decay isolines corresponding to $\tau_S = \tau_{\text{rec}}$ and $\tau_S = \tau_U$.

B. LSS formation bound

If $\tau_S > \tau_U$, the sterile neutrinos contribute to the dark matter in the Universe. Analysis of the large scale structure (LSS) of the Universe gives the bound on the total energy density in sterile neutrinos ρ_S as function of its mass:

$$\omega_S \equiv \frac{\rho_S}{\rho_{\text{cr}}} h^2 \leq \omega_S(m_S). \tag{40}$$

Here ρ_{cr} is the critical energy density and h is the Hubble constant.[1] We use for $\omega_S(m_S)$ the results of the analysis in [17,18].

For $m_S < 100$ eV, S compose the hot dark matter component and the bound on ω_S is stronger. According to [17] for $m_S < 30$ eV one has $\omega_S < 0.005$ at 95% CL. The bound weakens with the increase of m_S, as neutrinos become colder: $\omega_S < 0.02$ at $m_S = 100$ eV, and $\omega_S < 0.12$ at $m_S = 300$ eV. In the interval $m_S = (0.25 - 30)$ eV the 95% CL bound from [18] can be parametrized as

$$\omega_S \leq 0.001 \left[\left(\ln\left(\frac{m_S}{\text{eV}}\right) - 1.7 \right)^2 + 2.5 \right]. \tag{41}$$

For $m_S = (30{-}300)$ eV[2]:

$$\omega_S \leq 0.01 \left[\left(\ln\left(\frac{m_S}{\text{eV}}\right) - 2.55 \right)^{2.2} - 1.0 \right], \tag{42}$$

and $\omega_S < 0.12$ for $m_S > 300$ eV.

Calculations of the energy density ω_S have been updated recently [19] with inclusion of a number of additional effects, in particular, effects of the quark-hadron transition, modification of the finite temperature effective mass of the active neutrinos, etc. For the temperature of the quarks-hadron transition $T_{\text{QCD}} = 170$ MeV, the relation between ω_S, m_S, and θ_S can be parametrized as [19]

$$m_S = 1.45 \text{ keV} \left(\frac{10^{-8}}{\sin^2\theta_S}\right)^{0.615} \left(\frac{\omega_S(m_S)}{0.13}\right)^{0.5}, \tag{43}$$

or

$$\sin^2\theta_S = 1.83 \cdot 10^{-8} \left(\frac{\omega_S(m_S)}{0.13}\right)^{0.813} \left(\frac{1 \text{ keV}}{m_S}\right)^{1.626}. \tag{44}$$

Notice that for $m_S < 3$ keV it deviates from the dependence previously found in [20].

Plugging the limits (41) and (42) in relation (44) we find the upper bound on $\sin^2\theta_S$ as a function of m_S (see region LSS in Figs. 1–3). The bound is absent for $m_S < 0.25$ eV [21]. It does not depend on the flavor of active neutrino to which sterile neutrino mixes.

---

[1]In this paper in numerical estimations we use $h = 0.7$.

[2]A more accurate parametrization in this range is:

$$\omega_S \leq 6 \times 10^{-3} + 4.1 \times 10^{-6} \, (m_S/\text{eV}) + 2.5 \times 10^{-7} \, (m_S/\text{eV})^2$$
$$+ 1.7 \times 10^{-8} \, (m_S/\text{eV})^3 - 4.5 \times 10^{-11} \, (m_S/\text{eV})^4$$

The bound is valid for the region of parameters below the isoline $\tau_S = \tau_U$ which corresponds to $m_S < 0.5$ MeV and $\sin^2\theta_S > 7 \cdot 10^{-13}$. However for $m_S > 5$ keV the stronger bound follows from the diffuse background radiation.

It has been shown in a recent analysis [22] that sterile neutrinos with mass $m_S < 14$ keV are excluded at 95% CL as the dark matter particles responsible for the LSS formation. This implies a somehow stronger bound on ω_S than the one we use in our estimations and consequently stronger bound on the S parameters. It is argued that the bound can be relaxed if new particle decays in the epoch between the decoupling of S and big bang nucleosynthesis (BBN) increase the entropy, thus diluting concentration of S and reducing their relative temperature [23]. This may be the case for the model proposed in [24,25] where two heavy right-handed singlet neutrinos have masses above 1 GeV. (Explanation of LSS by S would probably require that S are produced at some high energy scales by processes that are not related to active-sterile neutrino oscillations [23].)

C. Limit from cosmic x-ray radiation

Because of mixing via the loop diagrams sterile neutrinos decay into an active neutrino and a photon: $S \to \nu_a \gamma$ with $E_\gamma \approx m_S/2$ and at the rate $\Gamma_\gamma \sim \alpha\Gamma_{3\nu}$. Therefore one expects to detect the photon emission line when looking at big concentrations of dark matter such as galaxy clusters.

The analyses of the x-ray emission from the Virgo cluster [26,27] give limits on the decay and therefore on the mixing of sterile neutrino: $\sin^2\theta_S < 2.6 \times 10^{-6} \, (m_S/\text{keV})^{-4}$. (This parametrization is valid for $m_S = (1{-}10)$ keV.) It is argued in [28] that the bound from Virgo is about 1–2 orders of magnitude weaker especially for low masses, $m_S < (5{-}8)$ MeV. However for $m_S = 10$ keV, relevant for this analysis (where x-ray bounds start to dominate over the LSS one), the bounds are comparable: $\sin^2\theta_S < 2.6 \times 10^{-10}$ [26] and $\sin^2\theta_S < 5.0 \times 10^{-10}$ [28]. At the same time a stronger limit has been obtained from an analysis of Coma cluster [28]:

$$\sin^2\theta_S < 2 \times 10^{-5} \left(\frac{m_S}{\text{keV}}\right)^{-5}. \tag{45}$$

The γ-flux from all possible sources could accumulate over the history of the Universe and be seen as a diffuse extragalactic background radiation (DEBRA). Apparently the flux from the radiative S decay should be smaller than the observed flux. In the range $m_S = (1{-}100)$ keV the DEBRA limit can be parametrized as [29]

$$\sin^2\theta_S < 3.1 \times 10^{-5} \left(\frac{m_S}{\text{keV}}\right)^{-5}. \tag{46}$$

This bound based on the data collected from the whole sky is weaker than the one given in (45). However, it does not depend on assumptions concerning clustering and there-

fore is considered to be more robust [29]. These limits are valid below the recombination line $\tau_S = \tau_{\rm rec}$.

The x-ray exclusion region shown in Figs. 1–3 has been obtained from the analysis of Coma cluster data as well as data on diffuse x-ray background (DEBRA) from HEAO-1 and XMM-Newton missions in [29]. We have also included the very recent bound from the diffuse x-ray spectrum of the Andromeda galaxy [30]. This is the most stringent limit in the range $m_S = (1\text{--}24)$ keV. For small masses, $m_S \lesssim 1$ keV, we use the limit from [31].

Note in Figs. 1–3 that the x-ray data reduces the parameter space allowed for warm dark matter to a very small region: $m_s = (1.7\text{--}3.5)$ keV for $\sin^2\theta_S \sim 10^{-9} - 10^{-8}$. Also most of the parameter region that can explain the origin of pulsar velocities is ruled out, remaining only a corner around $m_S \sim 2\text{--}4$ keV.

It was proposed in Ref. [26] to observe clusters of galaxies with Chandra and XMM-Newton observatories, in their high sensitivity range for x-ray photon detection of (1–10) keV. That will allow one to set the limit in the range $10^{-13} < \sin^2 2\theta_S < 10^{-5}$ for $m_S = (0.6\text{--}40)$ keV.

D. CMB bound

If the sterile neutrinos decay producing light neutrinos between the active neutrino decoupling time $\tau_\nu \sim 1$ s and the photon decoupling time $\tau_{\rm rec}$, this would increase the energy density of relativistic particles at $t \lesssim \tau_{\rm rec}$. The density is described by the effective number of neutrinos N_ν. That, in turn, affects the CMB angular power spectrum (acoustic peaks). The bounds on N_ν from observations were substantially improved during the last 5 years: $N_\nu < 13$ at 95% CL (BOOMERanG/MAXIMA) [32], $N_\nu < 8.3$ at 90% CL (WMAP data) [33], $N_\nu < 6.8\text{--}7.1$ at 95% CL (WMAP and LSS) [34–36], $N_\nu < 5.4$ at 95% CL (WMAP, LSS, and type Ia supernova data) [37].

With the help of considerations in Refs. [20,38], we get the "CMB" limit on the sterile neutrino parameters as a function of N_ν, which can be parametrized as

$$\left(\frac{m_S}{\rm keV}\right)^4 = 3 \times 10^{33}(N_\nu - 3)^{-2.87}\sin^2\theta_S. \qquad (47)$$

The combined analysis of the cosmological data on LSS, supernovas, and the CMB including 3 years result from WMAP [39] allows to put the bound $N_\nu < 3.74$ at 95% CL. Using these results and Eq. (47) we find the bound shown in Figs. 1–3. This limit is not valid above the line $\tau_S < \tau_\nu \sim 1$ s, which for $\sin^2\theta_S = 10^{-12}$ corresponds to $m_S = (400\text{--}500)$ MeV.

In the future, the PLANCK mission [40,41] will allow to strengthen the bound down to $N_\nu < 3.2$, while according to Ref. [41], the CMBPOL mission can achieve $N_\nu < 3.05$. This will further expand the excluded region, in particular, to larger values of m_S.

E. BBN bound

Apparently for one sterile neutrino the limit on the effective number of additional degrees of freedom during the epoch of BBN, $\Delta N_\nu = 1$ does not provide any bound since at most the equilibrium concentration of S can be produced in the scenarios under consideration. The limit $\Delta N_\nu \lesssim 1$ becomes relevant in the case of more than two sterile states.

For the low values of m_S we use the limits from [42] which for $\Delta N_\nu = 1$ can be parametrized as

$$m_S\sin^2\theta_S = 1.4 \text{ meV} \quad \text{for } \nu_e, \qquad (48)$$

$$m_S\sin^2\theta_S = 1.0 \text{ meV} \quad \text{for } \nu_\mu, \nu_\tau. \qquad (49)$$

For the high masses, $m_S = 10\text{--}200$ MeV, the exclusion region has the shape of a parallelogram [43]. The right boundary is basically given by

$$\sin^2\theta_S\left(\frac{m_S}{\rm keV}\right)^3 = 1.25 \times 10^{11},$$

which is the condition for the heavy neutrinos to be relativistic at decoupling so their number density is not Boltzmann suppressed and they can have an impact on BBN. The left boundary,

$$\left(\frac{m_S}{\rm keV}\right)^2\sin^2\theta_S < 6 \times 10^{-2},$$

can be simply understood as the condition that the energy density of the sterile neutrino is smaller (including also an entropy dilution factor 5) than the energy density of one light neutrino species at BBN.

F. Supernova neutrino bound

Two different bounds follow from observation of the antineutrino signal from SN1987A [44]. One is from $\bar\nu_e$-disappearance and the other from star cooling.

(1) The resonance conversion $\bar\nu_e \to \bar{S}$ can occur in the central regions of the star due to change of sign of the matter potential. That happens for the active-sterile system when the relative electron number density is $Y_e \sim 1/3$. For the mass range $m_S \sim (1\text{--}100)$ eV the adiabaticity condition can be fulfilled if $\sin^2\theta_S > 10^{-5}$. The adiabatic conversion leads to strong suppression of the $\bar\nu_e$ flux [3]. So, the observation of the $\bar\nu_e$ signal from SN1987A gives the bound on the oscillation parameters. In Figs. 1 and 2 we show the updated results obtained in Ref. [4].

(2) For large masses, m_S, the $(\nu_a \to S)$ oscillations as well as scattering lead to production of sterile neutrinos in the core of the collapsing star. If these neutrinos escape the core, they can lead to substantial energy loss. This, in turn, will shorten the neu-

trino burst and the energy released in $\bar{\nu}_e$ will be smaller [31,45].

Normal duration of the SN1987A neutrino burst excludes significant cooling effect which puts the bound on S parameters [43] shown in Figs. 1–3. Notice that the upper bound, $\sin^2\theta_S \lesssim 10^{-10}$, is slightly different for ν_e and ν_μ and ν_τ. If mixing is sufficiently large, the sterile neutrinos will be trapped inside the core, and the energy-loss argument is not applicable. This gives the lower bound of the excluded region $\sin^2\theta_S \lesssim 10^{-2}$. The mass range is restricted by the condition that S is produced inside the core.

Future detection of high statistics neutrino signal from a galactic supernova will allow to put stronger bounds. Indeed, another resonance in $\nu_e - S$ can occur in the outer regions of the star with normal chemical composition. The adiabaticity condition can be written as

$$\gamma = 10^2 \sin^2\theta_S \left(\frac{m_S}{10^{-3}\,\text{keV}}\right)^{3.3} \gg 1 \qquad (50)$$

which in fact is stronger than the cosmological bound in the range (0.01–0.1) keV. The adiabatic $\nu_e - S$ conversion leads to the disappearance of the ν_e-neutronization peak, and the modification of the signal during the cooling stage. In particular, in the case of normal mass hierarchy the electron neutrino flux at the Earth will be $F(\nu_e) = F^0(\nu_\mu)$ in the case of large 1-3 mixing and $F(\nu_e) = \cos^2\theta_{12}F^0(\nu_\mu)$ for very small 1-3 mixing [3].

In the eV mass range, sterile neutrinos can drive non-negligible $\nu_\mu \rightarrow \nu_e / \bar{\nu}_\mu \rightarrow \bar{\nu}_e$, $\bar{\nu}_\tau$ conversions at TeV energies by the Mikheyev-Smirnov-Wolfenstein (MSW) effect that can be constrained by future IceCube data [46].

G. Laboratory bounds

The laboratory bounds are typically much weaker than the astrophysical and cosmological ones. They are, however, more robust and turn out to be the main bounds if, for some reason (see Sec. IV B), the cosmological and astrophysical limits become inapplicable.

(1) *The $0\nu\beta\beta$ decay.* Introduction of active-sterile mixing (described by $m_{\alpha S}$) does not change the m_{ee} element of the whole 4×4 mass matrix (4). Therefore for light S: $m_S \ll 1/r_N$, where r_N is the typical size of nuclei, the rate of $0\nu\beta\beta$ decay in the lowest approximation is determined by m_{ee} and the effect of S is strongly suppressed.

However, the effect of S on the $0\nu\beta\beta$ decay increases with m_S. Let us consider this in more details. The $0\nu\beta\beta$ decay amplitude $A^{(S)}$ has two contributions associated to S: (i) from the induced mass $(m_I)_{ee}$ and exchange of light neutrinos, and (ii) from exchange of S and its mixing with ν_e. So, the amplitude of the decay can be written as

$$A^{(S)} \propto \frac{(m_I)_{ee}}{\bar{q}^2 - m_\nu^2} + \frac{m_S \sin^2\theta_{eS}}{\bar{q}^2 - m_S^2}, \qquad (51)$$

where $\bar{q} \sim 1/r_N$ is the effective momentum of the exchanged neutrino. As it can be inferred from the calculation presented in [47], $\bar{q} \approx 100$ MeV. In the denominator of (51) the parameter m_ν is the effective mass of light neutrinos and since $m_\nu \ll m_S$ it can be neglected. Taking into account that the induced mass $(m_I)_{ee} = -m_S \sin^2\theta_{eS}$ we can write, according to Eq. (51)), the total contribution of S to the effective Majorana mass as

$$m_{ee}^{(S)} = m_S \sin^2\theta_{eS} \left| 1 - \frac{\bar{q}^2}{\bar{q}^2 - m_S^2} \right|. \qquad (52)$$

If m_S is negligible the two contributions cancel each other leading to zero effect of S. If $m_S^2 \ll \bar{q}^2$, we find from (52)

$$m_{ee}^{(S)} = \sin^2\theta_{eS} \frac{m_S^3}{\bar{q}^2}. \qquad (53)$$

So, for light S, $m_S \ll 1/r_N$, $m_{ee}^{(S)} \rightarrow 0$ and the total effective Majorana mass is determined by the ee elements of the active neutrino mass matrix $(\mathbf{m_a})_{ee}$, in agreement with consideration in terms of 4×4 matrix.

For $m_S^2 \gg \bar{q}^2$, the second term in (52) can be neglected and the Majorana mass is given by the induced contribution (as in the usual seesaw mechanism):

$$m_{ee}^{(S)} = \sin^2\theta_{eS} m_S. \qquad (54)$$

In Fig. 1 we show the excluded region of the S parameters which corresponds to the upper bound $m_{ee} < 0.5$ eV obtained from studies of $0\nu\beta\beta$ decay of ^{76}Ge [48]. We assume that there is no cancellation between S contribution and $(\mathbf{m_a})_{ee}$. In general, cancellation reduces the excluded region. However, in our context, the cancellation cannot be strong. Indeed, according to our assumption (Sec. II A) the original active neutrino mass terms are below 1 eV. Therefore maximal contribution to the effective Majorana mass of electron neutrino is about 1 eV, and consequently, only the order of 1 eV contribution from the new neutrino state can be cancelled. That corresponds to the long-dashed line in Fig. 1.

As follows from Fig. 1 the double beta decay limit becomes relevant for high masses $m_S > 100$ MeV. Future neutrinoless double beta decay experiments [49] with sensitivity down to $m_{ee} < (0.01-0.03)$ eV will improve the bound on $\sin^2\theta_S$ by a factor 10–30.

(2) *The β decay.* The region $m_S \sim (0.1-10^3)$ keV and $\sin^2\theta_S \lesssim 10^{-3}-10^{-2}$ for $\nu_S - \nu_e$ mixing (Fig. 1) is excluded by the negative results of searches of kinks in the energy spectra of nuclear β decays [50].

(3) *Meson decays* can have contributions from sterile neutrinos which can modify the energy spectra of their decay products. In the $\nu_S - \nu_e$ channel, the best limit comes from precision measurements of the energy spectrum of e^+ in the decay $\pi^+ \rightarrow e^+ \nu_e$ [51]: $\sin^2\theta_S < 10^{-7}$ for $m_S = (50\text{--}130)$ MeV. In the $\nu_S - \nu_\mu$ channel, the bounds come from studies of the spectra of $\pi^\pm$ and $K^\pm$ decays at accelerators and in the atmosphere. The 90% CL excluded region (labeled as "Decays" in Fig. 2) is taken from Ref. [52]. It is the only bound which can compete with the cosmological and astrophysical limits in the range of large masses $m_S \sim (0.03\text{--}0.3)$ GeV.

In the near future, the studies of pion, muon, and kaon decays at MiniBooNE [53], MINOS [54], and K2K [55] experiments are expected to reach sensitivities of a few $\times 10^{-7}$ or less for the mixing if $m_S \sim 100$ MeV [52].

Oscillations of active to sterile neutrinos lead to the suppression of the neutral current interaction rate. In this connection, it has been proposed to study interactions of neutrinos from pion decays at rest with the superallowed neutral current reaction $\nu_x {}^{12}\text{C} \rightarrow \nu_x {}^{12}\text{C}^*$ [56]. The sensitivity of such an experiment can reach $\sin^2\theta_S \sim 10^{-2}$ for $m_S \sim 1$ eV.

(4) *The atmospheric neutrinos and K2K.* The combined analysis of the Super Kamiokande [57] and MACRO [58] results as well as the data from accelerator experiment K2K leads to the following 90% CL. bounds [4]: for the $\nu_e - \nu_S$ channel $\sin^2\theta_S < 10^{-2}$, in the interval $m_S = (0.01\text{--}0.1)$ eV (see Fig. 1); for the $\nu_\mu - \nu_S$ channel $\sin^2\theta_S < 0.04$ in the range $m_S = (0.1\text{--}1)$ eV (see Fig. 2); for the $\nu_\tau - \nu_S$ mixing $\sin^2\theta_S < 0.1$.

If the cosmological bound is invalid, the atmospheric bound becomes also relevant for larger masses, $m_S = (1\text{--}10)$ eV.

Sterile neutrino oscillations for $m_S \sim$ few eV have the oscillation length comparable to the Earth's radius at $E_\nu \sim 1$ TeV. In the future, IceCube [59] detection of atmospheric neutrinos can probably bring the limit on $\nu_e - \nu_S$ mixing down to $\sim 10^{-2}$ for $m_S \sim$ few eV [46].

It been suggested in Ref. [60] that showers generated by ultrahigh energy sterile neutrinos $(E_\nu \sim 10^6\text{--}10^{12}$ GeV) with $\sin^2\theta_S \sim 0.01\text{--}0.1$, may be distinguished from the ones generated by active neutrinos in experiments such as EUSO [61] or OWL [62], using the Earth as a filter, as proposed in Ref. [63] for neutralino showers. The mass range of m_S that can be tested by these experiments is determined by the mechanism of their production.

(5) *Reactor neutrino experiments* can set limits on the mixing $\bar\nu_e - \bar\nu_S$ by comparing expected with observed $\bar\nu_e$ flux. Bugey [64], CHOOZ [65], and Palo Verde [66] provide the main bound on $\bar\nu_e - $

$\bar\nu_S$ mixing, $\sin^2\theta_S \lesssim 0.01$ (90% CL.), in the range $m_S = (0.3\text{--}1)$ eV.

The forthcoming reactor experiment Double-CHOOZ and the proposed projects Kaska, Braidwood, and Angra [67], may be able to reach $\sin^2\theta_S \sim 5 \times 10^{-3}$ for $m_S = (0.03\text{--}0.7)$ eV [68]

(6) *Accelerator bounds.* The accelerator oscillation experiments CDHS [69], CCFR [70], NOMAD [71], and CHORUS [72] as well as LSND [8], KARMEN [73], provide with the bound on $\nu_\mu - S$ mixing in the range low mass range, $m_S > (1\text{--}100)$ eV. In particular, $\sin^2\theta_S < 7 \times 10^{-3}$ (90% CL) for $m_S > 10$ eV (see region labeled "Beam" in Fig. 2).

In Figs. 1 we show the forbidden region of the parameters (labeled "Reac. + Beam") from the combined analysis of these accelerator beam and reactor experiments in Ref. [4]. This result excludes the induced mass as the origin of the dominant structure in the low m_S domain.

In the high mass range, $m_S > 0.1$ GeV mixing with a heavy S leads to an effective violation of lepton universality and appearance of the flavor changing neutral currents. The nonobservation of these effects in experimental data permitted the authors of Ref. [74] to set the 90% CL limits, shown in Figs. 1–3: $\sin^2\theta_S < 7.1 \cdot 10^{-3}$ ($\nu_S - \nu_e$), valid in the range $m_S > 0.14$ GeV (m_π), $\sin^2\theta_S < 1.4 \times 10^{-3}$ ($\nu_S - \nu_\mu$), valid in the range $m_S > 1.115$ GeV (m_Λ), and $\sin^2\theta_S < 1.7 \times 10^{-2}$ ($\nu_S - \nu_\tau$), valid in the range $m_S > 1.777$ GeV (m_τ). Also searches for a singlet neutral heavy lepton at LEP [75] have allowed to exclude $\sin^2\theta_S$ down to $10^{-4}\text{--}10^{-1}$ depending on the channel, in the range $0.4 < m_S/\text{GeV} < 90$ at 95% CL.

Accelerator experiments sensitive to oscillations with $\Delta m^2 > \Delta m^2_{32}$ will be able to set stringent bounds in the low mass range. The MINOS detector [54] can use the neutral current to charged current ratio to probe $\nu_\mu - \nu_S$ and $\nu_\tau - \nu_S$ mixing down to $\sin^2\theta_S \sim 10^{-2}$ [4]. Sensitivity to $\nu_\mu - \nu_S$ mixing at the level $\sin^2\theta_S \sim 10^{-3}$ for $m_S = (0.03\text{--}0.3)$ eV can be reached by T2K [76], NOνA [77], and future ν factories looking for ν_μ, $\bar\nu_\mu$ disappearance.

Forthcoming pp and planned $e^+ e^-$ collider experiments can expand the excluded region of S parameters to larger masses. According to Ref. [78], the search for same-sign dilepton production mediated by a sterile neutrino S in $pp \rightarrow l^+ l'^+ X$ with $l, l' = e, \mu, \tau$, may be used to constrain $\sin^2\theta_S \lesssim 10^{-2}$ for $m_S = (0.1\text{--}2)$ TeV at the large hadron collider at CERN, provided a large integrated luminosity becomes available. It has been shown [79] that at an international linear collider with a center of mass energy $\sqrt{s} = 500$ GeV, one can look for single heavy S production through $e^+ e^- \rightarrow S\nu \rightarrow lW\nu$ with $l = e, \mu, \tau$. This has a sensitivity down to

$\sin^2\theta_S < 7 \times 10^{-3}$ for $m_S = (200\text{--}400)$ GeV. The same reaction at a future compact linear collider operating with $\sqrt{s} = 3$ TeV could be used to limit $\sin^2\theta_S < (2\text{--}6) \times 10^{-3}$ for $m_S = 1\text{--}2$ TeV [80]. Notice however, that these high mass bounds are essentially irrelevant in our context. Indeed, for $m_S > 1$ GeV and $\sin^2\theta_S > 10^{-3}$, the induced mass is $m_I > 1$ MeV. This means that the elements of the original active neutrino mass matrix should also be large $m_a > 1$ MeV, and it should be an extremely strong cancellation of the original and induced contributions to obtain phenomenologically acceptable masses of light neutrinos: $((\mathbf{m_a})_{ij} - (\mathbf{m_I})_{ij})/((\mathbf{m_a})_{ij} < 10^{-7}$.

Inversely, discovery of the S with relatively large mixing in high energy collisions will testify against the approach developed in this paper.

IV. INDUCED MASS VERSUS DIRECT MIXING EFFECTS

A. Bounds on induced mass

Confronting the lines of constant induced masses (33)–(35), with cosmological astrophysical and laboratory bounds in the $\sin^2\theta_S$–m_S plane we can conclude on the relative importance of the direct and indirect effects.

There are two regions of parameters in the $\sin^2\theta_S$–m_S plane, where the induced masses are more important than the effects of direct mixing. That is, in these regions substantial induced masses for the active neutrino mass matrix are not excluded by the existing bounds.

1. High mass region

$m_S \gtrsim 300$ MeV and $\sin^2\theta_S \lesssim 10^{-9}$. This region is restricted essentially by the CMB bound, meson decays, and SN1987A cooling. Future measurements can probably improve the bounds by about 1 order of magnitude from below.

Only for the $\nu_e - \nu_S$ channel, the neutrinoless double beta decay can probe the whole high mass region. Present bounds correspond essentially to the dominant contribution in the case of the degenerate spectrum.

For the other mixing channels, it is the induced mass which gives the bound on the parameters of the sterile neutrinos. Indeed, assuming that there is no strong cancellation of elements of the original active neutrino mass matrix $\mathbf{m_a}$ and $\mathbf{m_I}$, and taking the largest elements of matrices in Table I, we can write the bound

$$\sin^2\theta_S m_S \lesssim m^{\exp} \sim (0.5\text{--}1) \text{ eV}, \qquad (55)$$

which is clearly comparable to the neutrinoless double beta decay bound but now valid for all channels. This can be viewed as the forth benchmark line shown in Fig. 1–3.

Sterile neutrinos in this range can play some role in leptogenesis and the generation of the baryon asymmetry in the Universe [24,81].

Clearly contribution from this region is out of our control and this creates ambiguity in the implications of the mass and mixing results.

It is beyond the scope of this paper to discuss the possible origins of S with such a small mixing. Still one possibility looks rather interesting: if $m_S = (10^2\text{--}10^6)$ GeV (region where one may expect singlets related, e.g., to SUSY breaking), the required mixing is $\sin^2\theta_S = 10^{-15}\text{--}10^{-12}$. The latter can be related to the existence of a new "intermediate" scale $M = m_S/\sin\theta_S \sim (10^{10}\text{--}10^{12})$ GeV.

If the interpretation of the LSND result in terms of oscillations in $(3 + 1)$ scheme is confirmed, that would imply existence of the sterile neutrino(s) with mass $(0.5\text{--}5)$ eV with mixing parameters $\sin^2\theta_S \sim 0.02$ (see [82] for recent analysis). The corresponding induced mass equals $m_I = (10\text{--}100)$ meV and therefore the effects of LSND neutrino on the active neutrino mass matrix is strong and cannot be considered as small perturbation.

2. Low mass window

$m_S \sim (0.1\text{--}0.3)$ eV and $\sin^2\theta_S = 10^{-3}\text{--}10^{-1}$. This window is essentially closed for all the channels if one takes the BBN bound $\Delta N_\nu < 1$. In this case, one has the bound on the induced mass $m_I < 1$ meV. That can produce some effect on observables in the case of degenerate or inverted hierarchy spectrum. From above this region is restricted by the LSS bound on neutrino mass.

If $\Delta N_\nu = 1$ is allowed, there is no BBN bound. Bounds from other effects strongly depend on flavor. For the $\nu_e - \nu_S$ channel, the reactor and atmospheric neutrino bounds essentially exclude the dominant contribution from m_I but still allow for subdominant effects. For the $\nu_\mu - \nu_S$ channel, the bound is given essentially by the atmospheric neutrinos and larger region of mixings is allowed. In particular, for $m_S \sim 0.25$ eV the mixing $\sin^2\theta_S = 0.04$ is not excluded leading to $m_I \sim 10$ meV. The latter is close to the dominant contribution. For the $\nu_\tau - \nu_S$ channel, the atmospheric bound is weaker and dominant contributions from m_I are allowed: $m_I \sim (30\text{--}250)$ meV.

In the rest of the m_S region, $m_S = (10^{-3}\text{--}10^5)$ keV, effects of the direct mixing dominate over the induced matrix effects. In this range the induced masses

$$m_I \lesssim 4 \times 10^{-2} \text{ meV}, \qquad (56)$$

can produce only very small corrections to the active neutrino mass matrix. In the interval $m_S = (1\text{--}10^4)$ keV the bound is even stronger:

$$m_I \lesssim 10^{-2} \text{ meV}. \qquad (57)$$

If however the cosmological/astrophysical bounds are absent for some reason, a large range of parameters becomes allowed and the induced masses can reproduce the dominant structures of the active neutrino mass matrix in the whole range of m_S.

In Fig. 1–3 we show also regions of parameters which correspond to certain positive indications of the existence of sterile neutrinos: (1) overlapping regions of the warm dark matter and pulsar kick, (2) the LSND spot.

In the scenario [24] two neutrinos have masses $m_S \gtrsim 1$ GeV and their mixing is responsible for the mass matrix of light active neutrinos: $\mathbf{m_a} = \mathbf{m}_I$. The third sterile neutrino with mass $m_S \sim 1$ keV and mixing $\sin^2 \theta_S \sim 10^{-9}$–$10^{-8}$ can contribute substantially to warm dark matter (WDM) and explain pulsar kicks.

Apparently the WDM and pulsar kick regions are far below the benchmark lines and therefore the corresponding induced masses are negligible. Furthermore, the regions are disfavored by the cosmological and astrophysical observations. The WDM scenario can be recovered if the mixing is smaller then that indicated in the plot and some additional mechanism of generation of sterile neutrinos exists apart from mixing with active neutrinos.

In contrast, the LSND spot is in the range where the induced masses are of the order of dominant mass structures. So mixing with sterile neutrino cannot be considered as small perturbation of the original active neutrino structure. The LSND spot is essentially excluded by the cosmological data unless some new physics is added.

B. Avoiding bounds

Let us consider various possibilities which allow one to circumvent the bounds obtained in the previous section and therefore to open a possibility for strong effects of the induced matrix even for low m_S.

(1) It has been shown [60] that in a cosmological scenario with low reheating temperature at the end of inflation, $T_R \ll 100$ MeV, experimental bounds on the active-sterile neutrino mixing are relaxed. In particular, the sterile neutrino required to explain the LSND result is allowed in this scenario. Also the influence of a non-negligible primordial lepton number asymmetry has impact on the sterile production rate since in this case neutrinos are produced resonantly with a nonthermal spectrum [20,83,84]. According to Ref. [20], for $L = 10^{-3}$ the LSS limit presented in Figs. 1–3 will change very little, while for $L = 0.1$ the limit on $\sin^2 \theta_S$ can increase by 1 or 2 orders of magnitude depending on m_S.

(2) Another possibility can be related to the origin of the mass of S itself. Recall that S may not be related to right-handed neutrinos and usual family structure. Let us assume that S has a "soft mass" generated by the medium dependent vacuum expectation value (VEV) of some new scalar field A: $m_S = \lambda \langle A \rangle$. The VEV can be proportional to the number density of the active neutrinos, n_ν: $\langle A \rangle \propto n_\nu$ [85]. In this case

$$m_S = m_S^0 (1 + z)^3, \qquad (58)$$

where m_S^0 is the mass in the present epoch. If the mixing mass is generated by the usual Higgs VEV, which does not change with time, we find that the induced contribution to the light mass and the active-sterile mixing decrease back in time:

$$m_I = \frac{m_{iS}^2}{m_S^0 (1 + z)^3} = m_I^0 (1 + z)^{-3}, \qquad (59)$$

$$\sin \theta_S = \frac{m_{iS}}{m_S^0 (1 + z)^3} = \sin \theta_S^0 (1 + z)^{-3}. \qquad (60)$$

Here m_I^0 and θ_S^0 are parameters at the present epoch. The combination we plot in Figs. 1–3 changes as

$$\sin^2 \theta_S m_S = \frac{\sin^2 \theta_S^0 m_S^0}{(1 + z)^3}. \qquad (61)$$

The lines of constant induced mass shift with z to the left—to smaller masses and mixings. This means that in the past all cosmological bounds were satisfied.

Already at the recombination epoch the mass of sterile neutrino becomes of the order 10^4 GeV for the present mass $m_S^0 \sim 1$ eV and the mechanism of oscillation production does not work. Essentially, in this scenario the sterile neutrinos are not produced in the early Universe and their concentration is negligible. The astrophysical and cosmological bounds we have discussed are not applicable.

(3) If S interacts with a massless or low mass Majoron [86] ϕ, it can decay invisibly as $S \rightarrow \nu \phi$ or annihilate (see similar mechanism for the active neutrinos in [87]). If this decay is fast enough, $\tau_S \ll 1$ s, in principle, all astrophysical and cosmological bounds could be evaded. See [88] for the recent similar analysis. In the mass range $m_S \sim 1$ keV such a fast decay can be achieved for the scalar coupling $g \sim 10^{-8}$.

In the low mass range some restrictions on the off diagonal couplings $g\nu_a S\phi$ can be obtained from their effect on the freestreaming condition for active neutrinos. The latter should manifest itself in the precision measurements of the CMB acoustic peaks. One can use these bounds also for sterile neutrinos. In [89] a limit on the active neutrino coupling $g \lesssim 1 \times 10^{-11}(50 \text{ meV}/m_S)^2$ was obtained. According to Ref. [90], the limit is less severe and is absent if couplings with different active neutrinos are different, e.g., S has large coupling with ν_τ only.

V. CONCLUSIONS

The main conclusions of this paper can be summarized as follows.

(1) Mixing of the active neutrinos with sterile neutrinos, singlets of the SM symmetry group, generates an induced mass matrix of active neutrinos which can be the origin of peculiar properties of the lepton mixing and neutrino mass spectrum. It opens an alternative possibility to understand possible new symmetries in the neutrino sector. In this way, one can explain the substantial difference of mixing patterns of quarks and leptons.

Depending on masses and mixings of S, the induced active neutrino masses can be the origin of the dominant or subdominant structures of the neutrino mass matrix. For instance, the tribimaximal mixing can originate from the induced contribution.

(2) Apart from modification of the mass matrix of active neutrinos, there are direct mixing effects of S which can be observed in cosmology, astrophysics, and laboratory experiments.

The importance of the direct and induced effects depends on the range of S parameters considered. For $m_S \gtrsim 300$ MeV the induced effect dominates. The induced masses can reproduce the dominant structures of the active mass matrix. The direct mixing effects are negligible. In the interval $m_S \sim (10^{-3}$–$10^5)$ keV the direct mixing effects dominate: the astrophysical and cosmological consequences of mixing are more important putting strong upper bounds on the induced mass. So, the latter can be neglected in the mass matrix of active neutrinos. In the narrow window $m_S \sim (0.1$–$0.3)$ eV the two effects are comparable. For the BBN bound $\Delta N_\nu < 1$ the induced matrix can produce only small effects. If one additional neutrino is allowed by BBN, the induced masses can generate the subleading structures or even be comparable to the values of dominant mass matrix elements.

(3) New physics effects can relax or even lift the cosmological and astrophysical bounds thus opening a possibility to generate a large induced matrix in the whole range of masses $m_S > 0.01$ eV. Here interesting possibilities to notice are: cosmological scenarios with low reheating temperature, fast decay of S into a Majoron and neutrino, and the possibility of a soft mass m_S which varies with time, *a la* mass varying neutrino scenario.

[1] P. Minkowski, Phys. Lett. B **67**, 421 (1977); T. Yanagida, in *Proceedings of the Workshop on The Unified Theory and the Baryon Number in the Universe*, edited by O. Sawada and A. Sugamoto (KEK, Tsukuba, Japan, 1979), p. 95; S. L. Glashow, in *Proceedings of the 1979 Cargèse Summer Institute on Quarks and Leptons*, edited by M. Lévy, J.-L. Basdevant, D. Speiser, J. Weyers, R. Gastmans, and M. Jacob (Plenum, New York, 1980), p. 687; M. Gell-Mann, P. Ramond, and R. Slansky, *Supergravity* edited by P. van Nieuwenhuizen and D. Z. Freedman (North Holland, Amsterdam, 1979), p. 315; R. N. Mohapatra and G. Senjanović, Phys. Rev. Lett. **44**, 912 (1980).

[2] P. C. de Holanda and A. Y. Smirnov, Phys. Rev. D **69**, 113002 (2004); M. Sorel, J. M. Conrad, and M. Shaevitz, Phys. Rev. D **70**, 073004 (2004); M. C. Gonzalez-Garcia, M. Maltoni, and C. Pena-Garay, Phys. Rev. D **64**, 093001 (2001); W. Grimus and T. Schwetz, Eur. Phys. J. C **20**, 1 (2001); C. Giunti and M. Laveder, J. High Energy Phys. 102 (2001) 001; V. D. Barger *et al.*, Phys. Lett. B **489**, 345 (2000); S. Goswami, Phys. Rev. D **55**, 2931 (1997); J. J. Gomez-Cadenas and M. C. Gonzalez-Garcia, Z. Phys. C **71**, 443 (1996).

[3] O. L. G. Peres and A. Y. Smirnov, Nucl. Phys. **B599**, 3 (2001).

[4] M. Cirelli, *et al.*, Nucl. Phys. **B708**, 215 (2005).

[5] R. N. Mohapatra and S. Nussinov, Phys. Rev. D **60**, 013002 (1999).

[6] K. R. S. Balaji, A. Perez-Lorenzana, and A. Y. Smirnov, Phys. Lett. B **509**, 111 (2001).

[7] J. C. Gomez-Izquierdo and A. Perez-Lorenzana, hep-ph/0601223.

[8] A. Aguilar *et al.* (LSND Collaboration), Phys. Rev. D **64**, 112007 (2001).

[9] S. Dodelson and L. M. Widrow, Phys. Rev. Lett. **72**, 17 (1994).

[10] See A. D. Dolgov, Phys. Rep. **370**, 333 (2002), for a complete review of references.

[11] A. Kusenko and G. Segre, Phys. Lett. B **396**, 197 (1997); G. M. Fuller, A. Kusenko, I. Mocioiu, and S. Pascoli,

Phys. Rev. D **68**, 103002 (2003); A. Kusenko, Int. J. Mod. Phys. D **13**, 2065 (2004).

[12] P. L. Biermann and A. Kusenko, Phys. Rev. Lett. **96**, 091301 (2006).

[13] G. L. Fogli, E. Lisi, A. Marrone, and A. Palazzo, hep-ph/0506083.

[14] A. Y. Smirnov, in *Proceedings of the Workshop on Neutrino Oscillations, Venice, 2003*, edited by M. B. Ceolin (Istituto Nazionale di Fisica Nucleare, Padova, 2003); M. Raidal, Phys. Rev. Lett. **93**, 161801 (2004); H. Minakata and A. Y. Smirnov, Phys. Rev. D **70**, 073009 (2004).

[15] K. Enqvist, K. Kainulainen, and M. J. Thomson, Nucl. Phys. **B373**, 498 (1992).

[16] X. Shi, D. N. Schramm, and B. D. Fields, Phys. Rev. D **48**, 2563 (1993).

[17] S. Dodelson, A. Melchiorri, and A. Slosar, astro-ph/0511500.

[18] A. Slosar (private communication).

[19] K. Abazajian, Phys. Rev. D **73**, 063506 (2006).

[20] K. Abazajian, G. M. Fuller, and M. Patel, Phys. Rev. D **64**, 023501 (2001).

[21] U. Seljak, A. Solar, and P. McDonald, astro-ph/0604335.

[22] U. Seljak, A. Makarov, P. McDonald, and H. Trac, astro-ph/0602430.

[23] T. Asaka, A. Kusenko, and M. Shaposhnikov, hep-ph/0602150.

[24] T. Asaka and M. Shaposhnikov, Phys. Lett. B **620**, 17 (2005).

[25] T. Asaka, S. Blanchet, and M. Shaposhnikov, Phys. Lett. B **631**, 151 (2005).

[26] K. Abazajian, G. M. Fuller, and W. H. Tucker, Astrophys. J. **562**, 593 (2001).

[27] M. Mapelli and A. Ferrara, Mon. Not. R. Astron. Soc. **364**, 2 (2005).

[28] A. Boyarsky, A. Neronov, O. Ruchayskiy, and M. Shaposhnikov, astro-ph/0603368.

[29] A. Boyarsky, A. Neronov, O. Ruchayskiy, and M. Shaposhnikov, astro-ph/0512509.

[30] C. R. Watson, J. F. Beacom, H. Yüksel, and T. P. Walker, astro-ph/0605424.

[31] A. D. Dolgov and S. H. Hansen, Astropart. Phys. **16**, 339 (2002).

[32] P. de Bernardis *et al.* (Boomerang Collaboration), Nature (London) **404**, 955 (2000); A. Balbi *et al.*, Astrophys. J. **545**, L1 (2000); **558**, L145(E) (2001).

[33] V. Barger, J. P. Kneller, H. S. Lee, D. Marfatia, and G. Steigman, Phys. Lett. B **566**, 8 (2003).

[34] P. Crotty, J. Lesgourgues, and S. Pastor, Phys. Rev. D **67**, 123005 (2003).

[35] E. Pierpaoli, Mon. Not. R. Astron. Soc. **342**, L63 (2003).

[36] S. Hannestad, J. Cosmol. Astropart. Phys. 05 (2003) 004.

[37] S. Hannestad, J. Cosmol. Astropart. Phys. 01 (2006) 001.

[38] S. Hannestad and G. Raffelt, Phys. Rev. D **59**, 043001 (1998).

[39] D. N. Spergel *et al.*, astro-ph/0603449.

[40] R. Bowen, S. H. Hansen, A. Melchiorri, J. Silk, and R. Trotta, Mon. Not. R. Astron. Soc. **334**, 760 (2002).

[41] S. Bashinsky and U. Seljak, Phys. Rev. D **69**, 083002 (2004).

[42] A. D. Dolgov and F. L. Villante, Nucl. Phys. **B679**, 261 (2004).

[43] A. D. Dolgov, S. H. Hansen, G. Raffelt, and D. V. Semikoz, Nucl. Phys. **B590**, 562 (2000).

[44] K. Hirata *et al.* (KAMIOKANDE-II Collaboration), Phys. Rev. Lett. **58**, 1490 (1987); J. C. Van Der Velde *et al.* (IMB Collaboration), Nucl. Instrum. Methods Phys. Res., Sect. A **264**, 28 (1988).

[45] K. Kainulainen, J. Maalampi, and J. T. Peltoniemi, Nucl. Phys. **B358**, 435 (1991).

[46] H. Nunokawa, O. L. G. Peres, and R. Zukanovich Funchal, Phys. Lett. B **562**, 279 (2003).

[47] P. Benes, A. Faessler, F. Simkovic, and S. Kovalenko, Phys. Rev. D **71**, 077901 (2005).

[48] H. V. Klapdor-Kleingrothaus *et al.*, Eur. Phys. J. A **12**, 147 (2001); C. E. Aalseth *et al.*, Phys. Rev. D **65**, 092007 (2002).

[49] C. Arnaboldi *et al.* (CUORE Collaboration), Astropart. Phys. **20**, 91 (2003); M. Danilov *et al.* (EXO Collaboration), Phys. Lett. B **480**, 12 (2000); C. E. Aalseth *et al.* (Majorana Collaboration), Phys. At. Nucl. **67**, 2002 (2004); H. Ejiri *et al.* (MOON Collaboration), Phys. Rev. Lett. **85**, 2917 (2000); K. Zuber (COBRA Collaboration), Phys. Lett. B **519**, 1 (2001); N. Ishihara, T. Ohama, and Y. Yamada (DCBA Collaboration), Nucl. Instrum. Methods Phys. Res., Sect. A **373**, 325 (1996); S. Yoshida *et al.* (CANDLES Collaboration), Nucl. Phys. B, Proc. Suppl. **138**, 214 (2005); G. Bellini *et al.* (CAMEO Collaboration), Eur. Phys. J. C **19**, 43 (2001); I. Abt *et al.* (GERDA Collaboration), hep-ex/0404039; A. S. Barabash (NEMO Collaboration), hep-ex/0602011.

[50] K. Hagiwara *et al.*, Phys. Rev. D **66**, 010001 (2002).

[51] D. I. Britton *et al.*, Phys. Rev. D **49**, 28 (1994); D. A. Bryman and T. Numao, Phys. Rev. D **53**, 558 (1996).

[52] A. Kusenko, S. Pascoli, and D. Semikoz, J. High Energy Phys. 11 (2005) 028.

[53] E. Church *et al.* (BooNe Collaboration), FERMILAB Report No. FERMILAB-PROPOSAL-0898.

[54] C. B. Smith (MINOS Collaboration), Int. J. Mod. Phys. A **20**, 3059 (2005).

[55] T. Maruyama, Nucl. Instrum. Methods Phys. Res., Sect. A **503**, 118 (2003).

[56] G. T. Garvey *et al.*, Phys. Rev. D **72**, 092001 (2005).

[57] Y. Fukuda *et al.* (Super-Kamiokande Collaboration), Phys. Rev. Lett. **81**, 1562 (1998).

[58] M. Ambrosio *et al.* (MACRO Collaboration), Phys. Lett. B **566**, 35 (2003).

[59] J. Ahrens *et al.* (The IceCube Collaboration), Nucl. Phys. B, Proc. Suppl. **118**, 388 (2003).

[60] G. Gelmini, S. Palomares-Ruiz, and S. Pascoli, Phys. Rev. Lett. **93**, 081302 (2004).

[61] G. D'Ali Staiti (EUSO Collaboration), Nucl. Phys. B, Proc. Suppl. **136**, 415 (2004).

[62] Y. Takahashi (OWL Collaboration), in Proceedings of the Workshop on Observing Giant Cosmic Ray Air Showers for >10**20 eV Particles from Space, College Park, MD, 1997 (unpublished).

[63] C. Barbot *et al.*, Phys. Lett. B **563**, 132 (2003).

[64] Y. Declais *et al.*, Nucl. Phys. **B434**, 503 (1995).

[65] M. Apollonio *et al.* (CHOOZ Collaboration), Phys. Lett. B **466**, 415 (1999).

[66] F. Boehm *et al.*, Phys. Rev. D **62**, 072002 (2000).

[67] K. Anderson *et al.*, hep-ex/0402041.

[68] V. Kopeikin, L. Mikaelyan, and V. Sinev, hep-ph/0310246.

[69] F. Dydak *et al.*, Phys. Lett. B **134**, 281 (1984).

[70] I. E. Stockdale *et al.*, Phys. Rev. Lett. **52**, 1384 (1984).

[71] P. Astier *et al.* (NOMAD Collaboration), Nucl. Phys. **B611**, 3 (2001).

[72] E. Eskut *et al.* (CHORUS Collaboration), Phys. Lett. B **497**, 8 (2001).

[73] B. Armbruster *et al.* (KARMEN Collaboration), Phys. Rev. D **65**, 112001 (2002).

[74] E. Nardi, E. Roulet, and D. Tommasini, Phys. Lett. B **327**, 319 (1994).

[75] O. Adriani *et al.* (L3 Collaboration), Phys. Lett. B **295**, 371 (1992).

[76] Y. Itow *et al.*, hep-ex/0106019.

[77] D. S. Ayres *et al.* (NOvA Collaboration), hep-ex/0503053.

[78] A. Ali, A. V. Borisov, and N. B. Zamorin, Eur. Phys. J. C **21**, 123 (2001).

[79] F. del Aguila, J. A. Aguilar-Saavedra, A. Martinez de la Ossa, and D. Meloni, Phys. Lett. B **613**, 170 (2005).

[80] F. del Aguila and J. A. Aguilar-Saavedra, J. High Energy Phys. 05 (2005) 026.

[81] E. K. Akhmedov, V. A. Rubakov, and A. Y. Smirnov, Phys. Rev. Lett. **81**, 1359 (1998).

[82] S. Goswami and W. Rodejohann, hep-ph/0512234.

[83] X. Shi and G. M. Fuller, Phys. Rev. Lett. **82**, 2832 (1999).

[84] K. Abazajian, N. F. Bell, G. M. Fuller, and Y. Y. Y. Wong, Phys. Rev. D **72**, 063004 (2005).

[85] R. Fardon, A. E. Nelson, and N. Weiner, J. Cosmol. Astropart. Phys. 10 (2004) 005.

[86] Y. Chikashige, R. N. Mohapatra, and R. D. Peccei, Phys. Lett. B **98**, 265 (1981); J. Schechter and J. W. F. Valle, Phys. Rev. D **25**, 774 (1982); G. Gelmini and E. Roulet, Rep. Prog. Phys. **58**, 1207 (1995).

[87] J. F. Beacom, N. F. Bell, and S. Dodelson, Phys. Rev. Lett. **93**, 121302 (2004).

[88] S. Palomares-Ruiz, S. Pascoli, and T. Schwetz, J. High Energy Phys. 09 048 (2005).

[89] S. Hannestad and G. Raffelt, Phys. Rev. D **72**, 103514 (2005).

[90] N. F. Bell, E. Pierpaoli, and K. Sigurdson, Phys. Rev. D **73**, 063523 (2006).